Electronic Supplementary Material (ESI) for Journal of Materials Chemistry A.

Supplementary Information

Enhanced oxygen evolution reaction of defective CoP/MOF-integrated electrocatalyst by partial phosphating

Zehua Zou [a], Junling Wang [b], Hairui Pan [a], Jian Li [a], Kailu Guo [a], Yongqing Zhao [a], Cailing Xu [a]*

[a]State Key Laboratory of Applied Organic Chemistry, Laboratory of Special Function Materials and Structure Design of the Ministry of Education, College of Chemistry and Chemical Engineering, Lanzhou University, Lanzhou 730000, China

[b]No. Sixteen Middle School, Lanzhou 730000, China

Experimental section

Chemicals

All chemical materials were used without further purification. $Co(NO_3)_2·6H_2O$ (≥98.5%, Xilong Scientific), $Cu(NO_3)_2·3H_2O$ (99.0~102.0%, Kermel), 4,5-Imidazoledicarboxylic acid (≥97.0%, Sigma-aldrich), NaOH (≥96.0%, Tianjin Damao), Sulfur sublimed (≥99.5%, Kermel), Selenium powder (≥99.7%, Zhongqin), 1,4-benzenedicarboxylic acid (≥98.5%, Guangfu), N,N-dimethylformamide (≥99.5%, Rionlon), Ethanol (≥99.7%, Rionlon) and $NaH_2PO_2·H_2O$ (≥98.0%, Kermel). The deionized water (DI-water) was used throughout the synthesis.

Synthesis of CoCu-MOF

$Co(NO_3)_2·6H_2O$ (0.57 mmol, 0.1657 g) and $Cu(NO_3)_2·3H_2O$ (0.03 mmol, 0.0072g) were dissolved in DI-water (20 mL) (Solution A). 4,5-Imidazoledicarboxylic acid (0.6 mmol, 0.0936 g) was deprotonated in NaOH solution (28 mL, 0.03 M) (Solution B). Then Solution B was quickly injected into Solution A under vigorous magnetic agitation. After stirring for 2 h, the precipitate was collected and washed with DI-water for several times by centrifugation and further dried overnight at 60 ^oC. For comparison, Co-MOF was prepared at the same condition except without addition of $Cu(NO_3)_2·3H_2O$.

Synthesis of D-CoCu-MOF-300

The obtained CoCu-MOF (0.0300 g) was placed in the porcelain boat and annealed at 300 ℃ for 1 h with a heating rate of 5 ℃ min^{-1} under flowing N_2 atmosphere. For comparison, D-CoCu-MOF-220 and Co_3O_4/D-CoCu-MOF-380 were prepared only by changing the annealing temperature of 220 ℃ and 380 ℃, respectively.

Synthesis of CoP/D-CoCu-MOF-300

In a typical process, the obtained D-CoCu-MOF-300 (0.0300 g) was placed in the porcelain boat at the downstream side and $NaH_2PO_2·H_2O$ (0.6000 g) was placed in another porcelain boat at the upstream side. The annealing treatment was set as 300 ℃ for 1 h with a heating rate of 5 ℃ min^{-1} under flowing N_2 atmosphere. For comparison, CoP/CoCu-MOF, CoP/D-CoCu-MOF-220 and CoP/$(CoCu)_2P_4O_{12}$ were prepared at the same condition only using different precursor (CoCu-MOF, D-CoCu-MOF-220 and Co_3O_4/D-CoCu-MOF-380, respectively). And the S-D-CoCu-MOF or S-CoCu-MOF was used Sulfur sublimed (0.600 g) as sulfur source, while Se-D-CoCu-MOF or Se-CoCu-MOF were prepared and so on.

Synthesis of P-D-Co-BDC

The Co-BDC MOFs were prepared according to the reference.[1] Then the P-D-Co-BDC powder was prepared referring to the synthesis of CoP/D-CoCu-MOF-300, except that the presintering temperature was chosen as 420 ℃.

Characterization

Thermogravimetric (TG) curves were measured on a thermogravimetric analysis instrument (Netzsch STA 449C), with a heating rate of 5 ℃ min^{-1} from 25 to 750 ℃ under N_2 atmosphere. The X-ray diffraction (XRD) patterns were recorded on a X-ray

generator diffractometer (Rigaku D/max 2400). Scanning electron microscope (SEM) images and energy dispersive X-ray spectroscopy (SEM-EDS) spectra were photographed on a scanning electron microscope （thermoscientific Apero S). Transmission electron microscope (TEM) images, high resolution TEM (HRTEM) images and energy dispersive X-ray spectroscopy (EDS) mapping were observed on a transmission electron microscope (Philips TecnaiTM G2 F30). Fourier transform infrared spectroscopy (FTIR) spectra were recorded by a spectrometer (Bruker VERTEX 70v FT-IR). The X-ray photoelectron spectroscopy (XPS) spectra were obtained on a spectrophotometer (PHI-5702, C 1s at 284.5 eV).

Electrochemical measurements

Electrochemical measurements were conducted on a potentiostat electrochemical workstation (Metrohm, Autolab PGSTAT302N) in 1.0 M KOH solution. A standard three-electrode electrochemical setup was used: a glass carbon (GC, φ=3.0 mm) substrate electrode for the working electrode, a Hg/HgO electrode with 1.0 m KOH filling solution for reference electrodes and a graphite rod for counter electrodes, respectively. The catalyst ink was using 2.5 mg electrocatalyst and 20 μL 5 wt% Nafion solutions, dispersed them into 1 mL of DI-water, and treated with an ultrasonic treatment to form a homogeneous slurry. Then, 6.0 μL as-prepared catalyst ink was deposited onto the clean surface of GC electrode, and the loading is calculated as 0.212 mg cm^{-2}. The potentials vs. Hg/HgO were converted to the reversible hydrogen electrode by using $E_{(RHE)} = E_{(Hg/HgO)} + 0.0591\ pH + 0.098$.

The polarization curves were measured by linear sweep voltammetry (LSV) at a scan rate of 5.0 mV s^{-1} in the range from 0 to 0.9 V vs Hg/HgO at room temperature. The current density was normalized by the geometric surface area of GC electrode. The electrochemical impedance spectroscopy (EIS) test was measured at a potential of 1.53 V vs RHE, in a frequency range of 0.1-100k Hz with an amplitude of 5.0 mV.

The overpotential was calculated using $\eta = E(RHE) - 1.23$.

Mass activity $J_m = j_{geo}/m$. Where j_{geo} is the measured current at a certain overpotential of 300 mV, and m is the loading mass.

Reference

1 G. Hai, X. Jia, K. Zhang, X. Liu, Z. Wu and G. Wang, High-performance oxygen evolution catalyst using two-dimensional ultrathin metal-organic frameworks nanosheets, *Nano Energy*, 2018, **44**, 345-352.

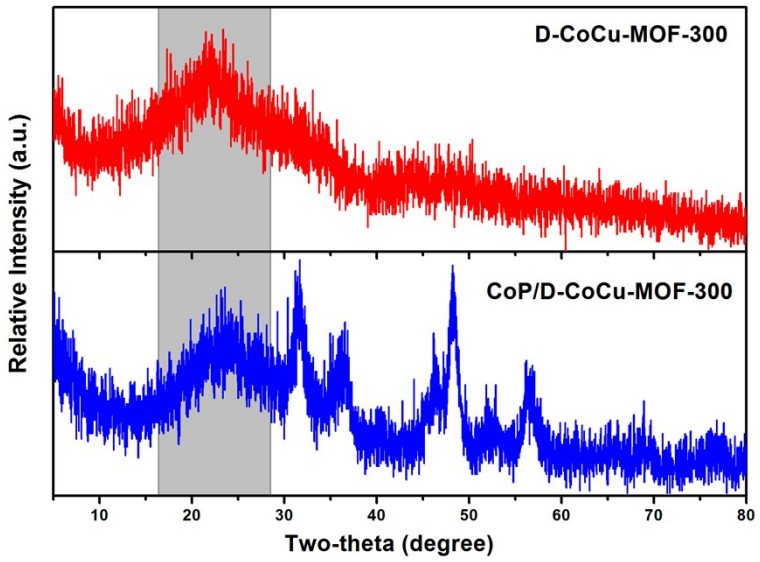

Fig. S1. The XRD patterns of D-CoCu-MOF-300 and CoP/D-CoCu-MOF-300.

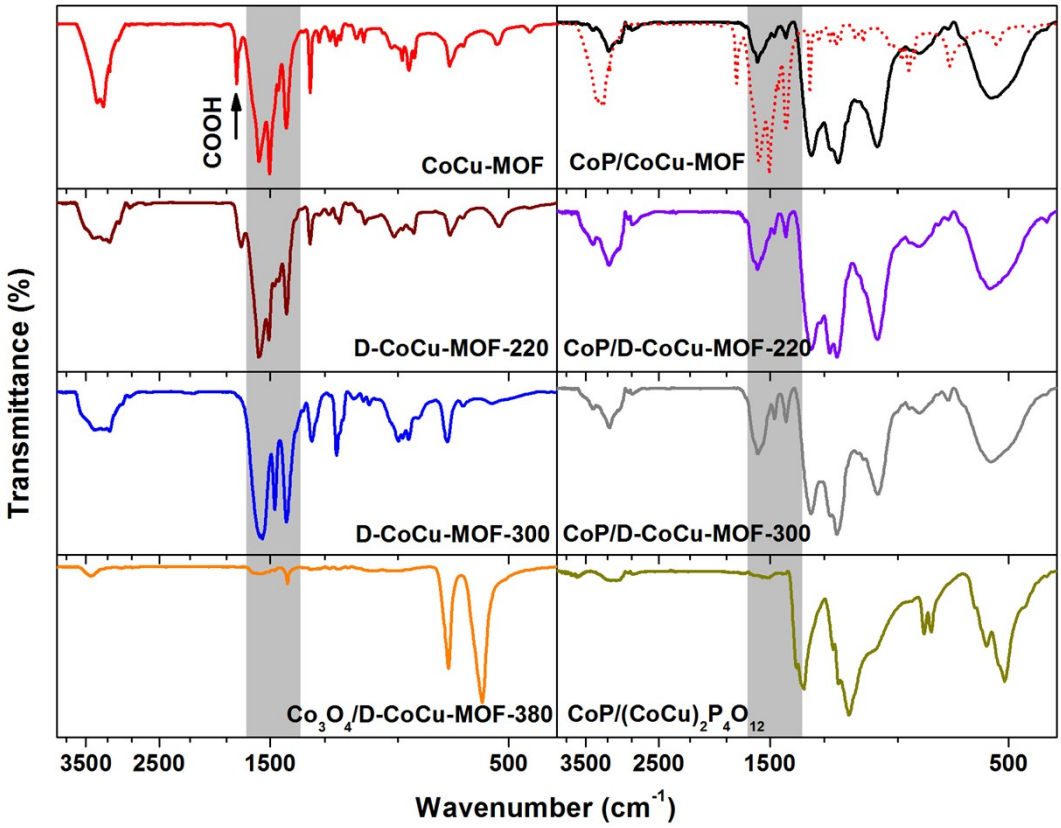

Fig. S2. The FT-IR spectra of CoCu-MOF, CoP/CoCu-MOF, D-CoCu-MOF-220, CoP/D-CoCu-MOF-220, D-CoCu-MOF-300, CoP/D-CoCu-MOF-300, Co_3O_4/D-CoCu-MOF-380 and CoP/$(CoCu)_2P_4O_{12}$. The red dashed corresponding to the spectrum of CoCu-MOF for comparative purposes.

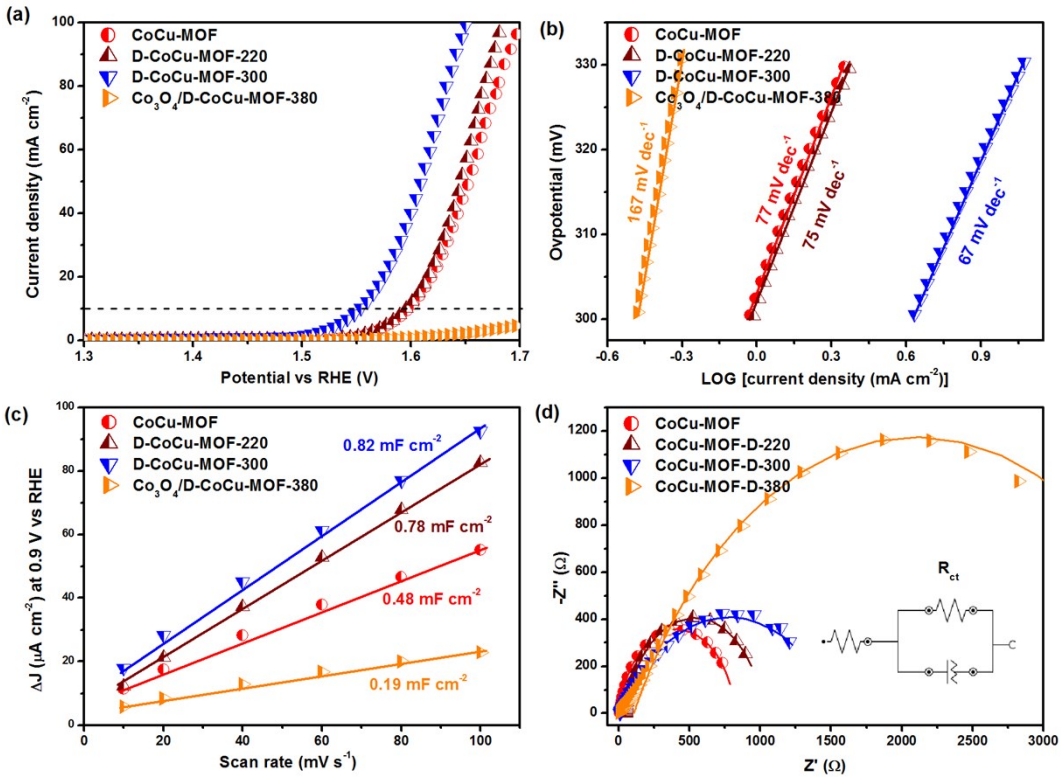

Fig. S3. (a) The LSV, (b) Tafel, (c) C_{dl} and (d) EIS curves of CoCu-MOF, D-CoCu-MOF-220, D-CoCu-MOF-300 and Co_3O_4/D-CoCu-MOF-380, respectively. Inset: the equivalent circuit.

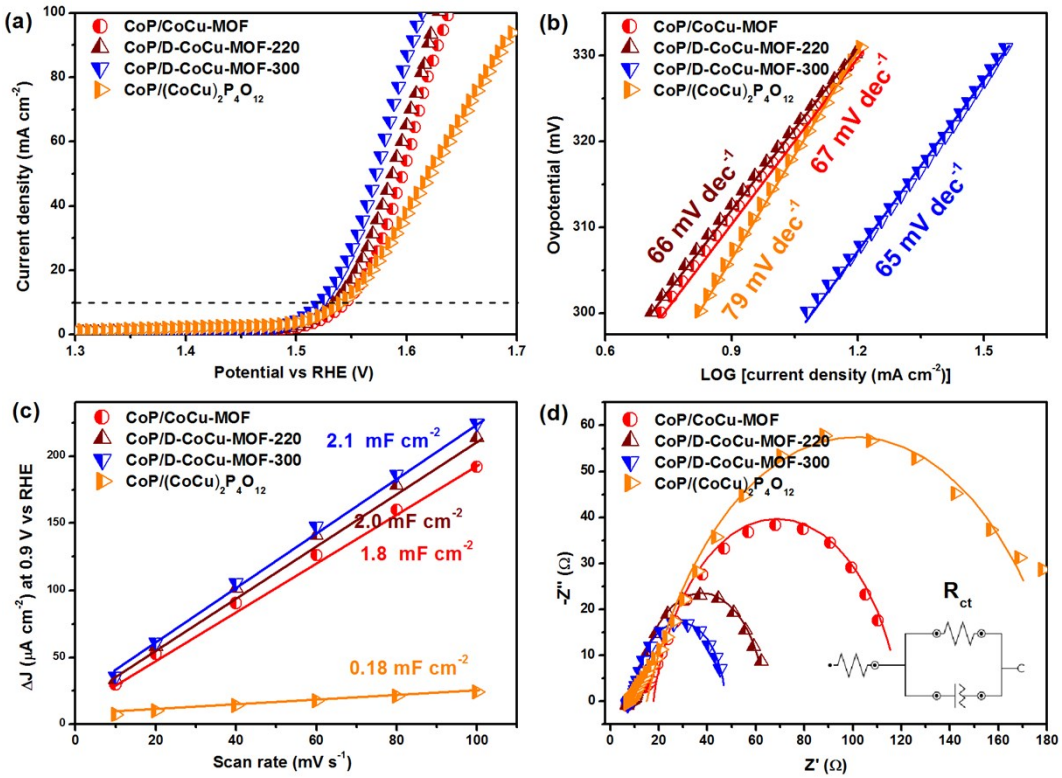

Fig. S4. (a) The LSV, (b) Tafel, (c) C_{dl} and (d) EIS curves of CoP/CoCu-MOF, CoP/D-CoCu-MOF-220, CoP/D-CoCu-MOF-300 and CoP/$(CoCu)_2P_4O_{12}$, respectively. Inset: the equivalent circuit.

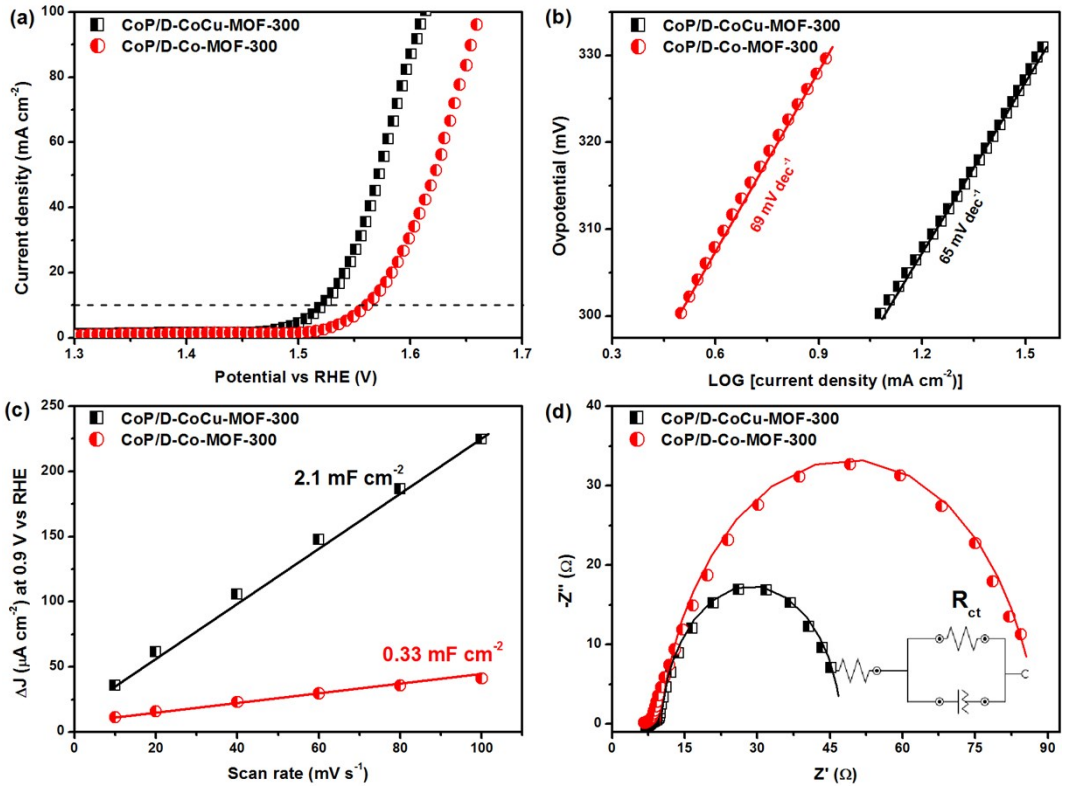

Fig. S5. (a) The LSV, (b) Tafel, (c) C_{dl} and (d) EIS curves of CoP/D-CoCu-MOF-300 and CoP/D-Co-MOF-300, respectively.

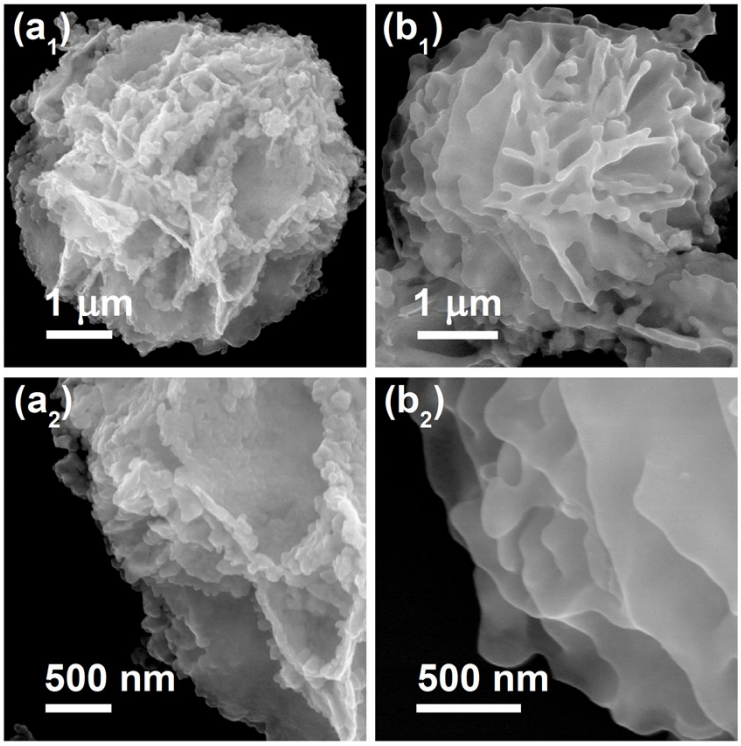

Fig. S6. The SEM images of (a) Co_3O_4/D-CoCu-MOF-380 and (b) CoP/$(CoCu)_2P_4O_{12}$.

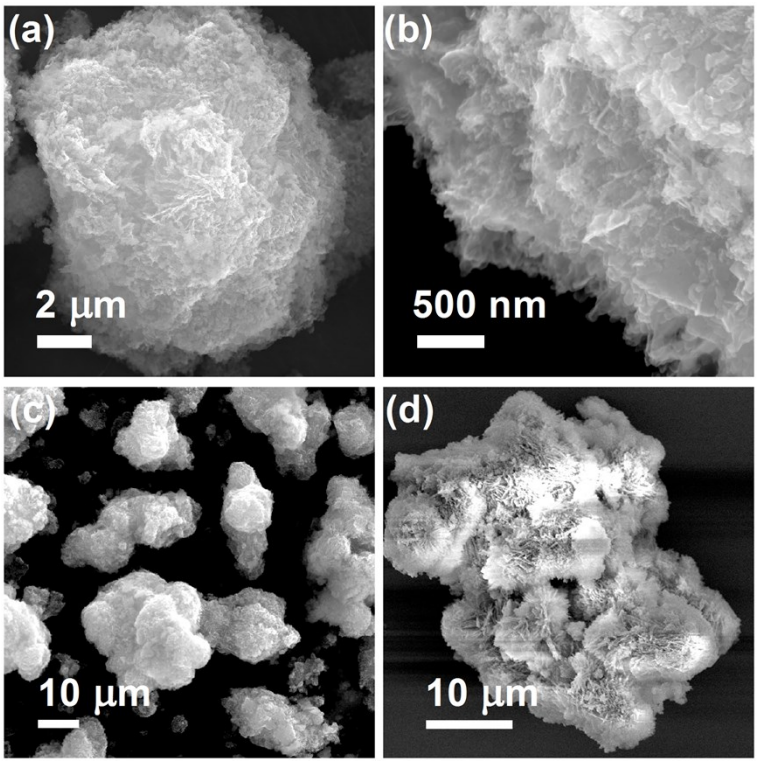

Fig. S7. The SEM images CoP/D-Co-MOF-300 at different magnification (a-c), at low test voltage (d).

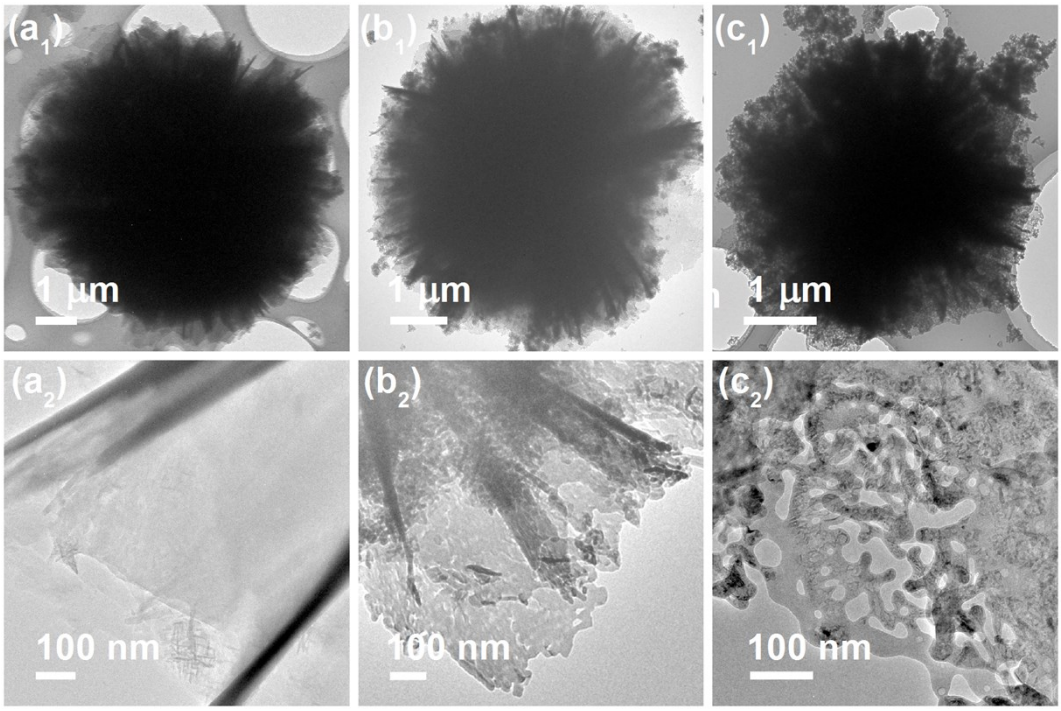

Fig. S8. The TEM images of (a) CoCu-MOF, (b) D-CoCu-MOF-300 and (c) CoP/CoCu-MOF.

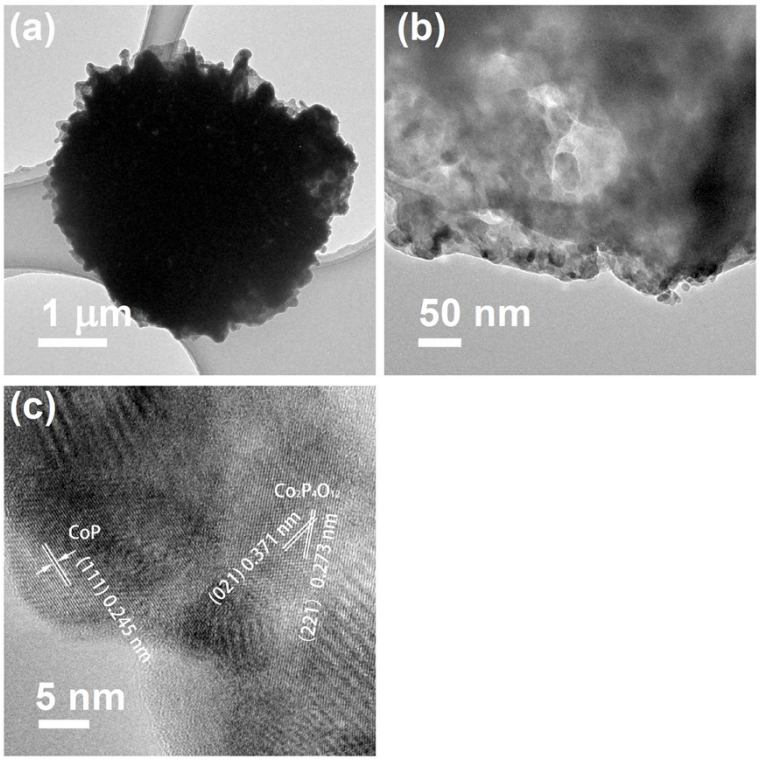

Fig. S9. The TEM images (a, b) and HRTEM images (c) of CoP/$(CoCu)_2P_4O_{12}$

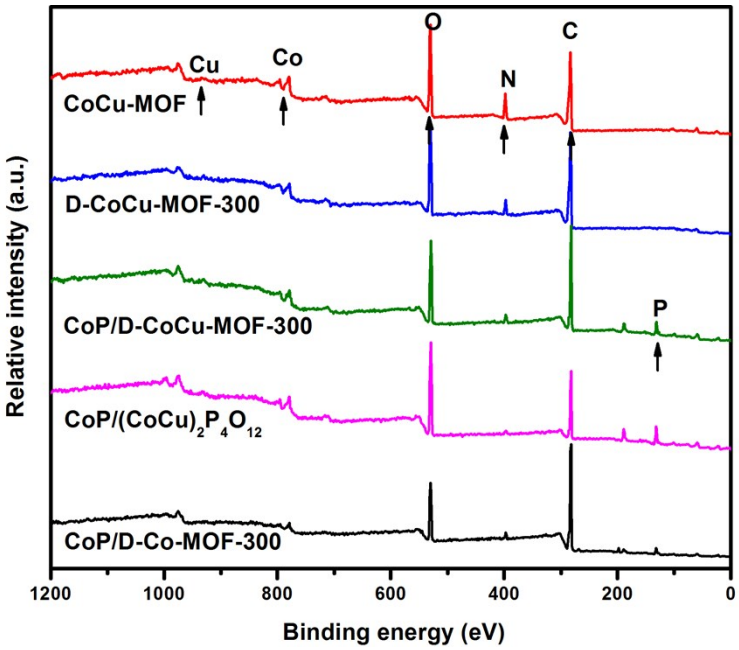

Fig. S10. The XPS spectra of CoCu-MOF, D-CoCu-MOF-300, CoP/D-CoCu-MOF-300, CoP/$(CoCu)_2P_4O_{12}$ and CoP/D-Co-MOF-300.

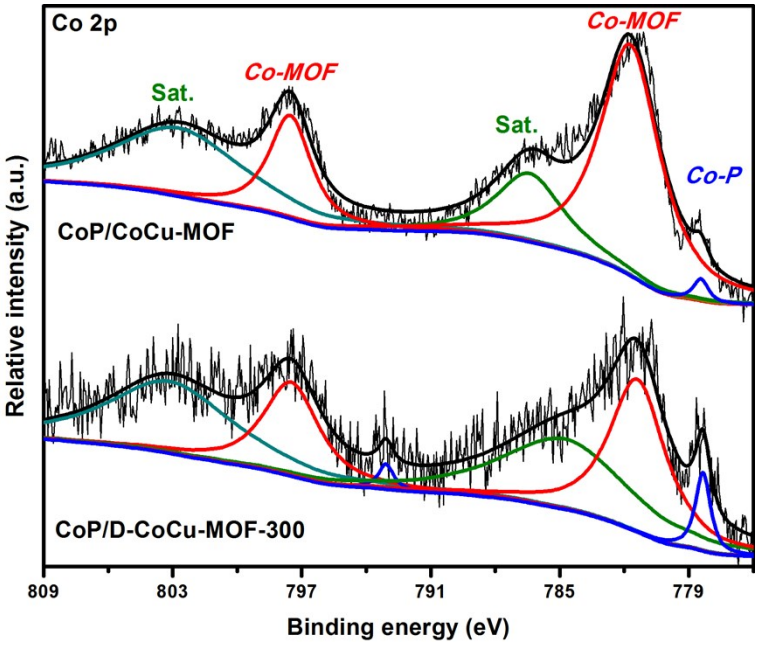

Fig. S11. The XPS spectra of Co 2p for CoP/CoCu-MOF and CoP/D-CoCu-MOF-300.

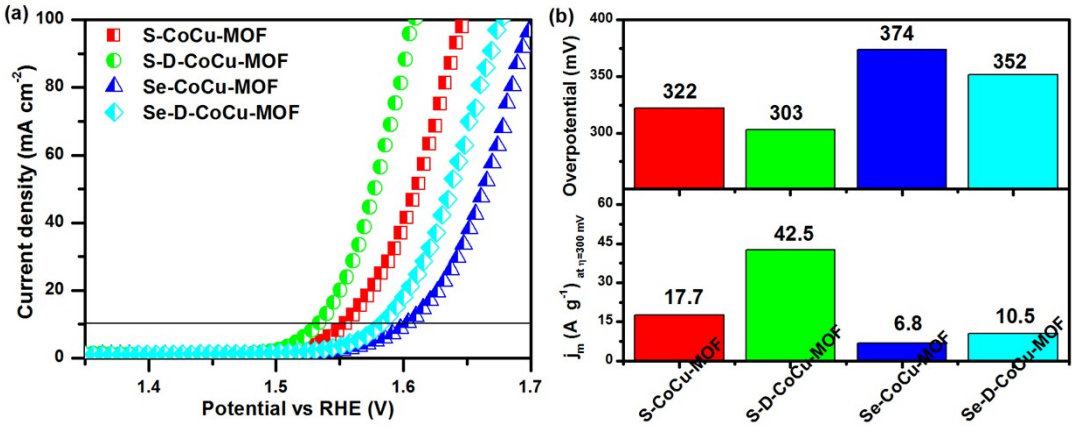

Fig. S12. (a) The LSV curves and (b) comparison of overpotential and mass activity for S-CoCu-MOF, S-D-CoCu-MOF, Se-CoCu-MOF and Se-D-CoCu-MOF, respectively.

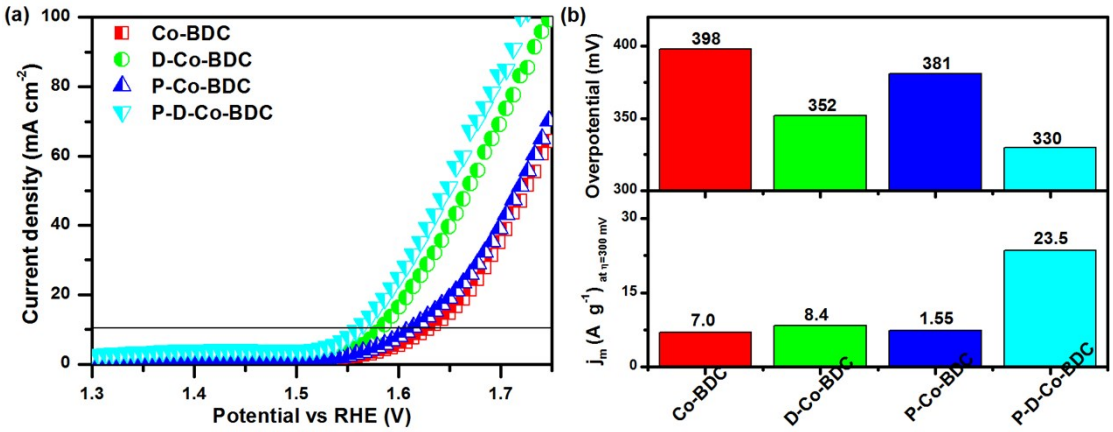

Fig. S13. (a) The LSV curves and (b) comparison of overpotential and mass activity for Co-BDC, D-Co-BDC, P-Co-BDC and P-D-Co-BDC, respectively.